Molecular Pharmacology Fast Forward. Published on July 6, 2006 as doi:10.1124/mol.106.025643

MOL 25643

The bioreduction of a series of benzoquinone ansamycins by NAD(P)H:quinone oxidoreductase 1 (NQO1) to more potent heat shock protein 90 (Hsp90) inhibitors, the hydroquinone ansamycins

Wenchang Guo†, Philip Reigan†, David Siegel, Joseph Zirrolli, Daniel Gustafson, and David Ross

Department of Pharmaceutical Sciences, School of Pharmacy and Cancer Center, University of Colorado Health Sciences Center, Denver, CO 80262 USA

Molecular Pharmacology Fast Forward. Published on July 6, 2006 as DOI: 10.1124/mol.106.025643
This article has not been copyedited and formatted. The final version may differ from this version.

MOL 25643

Running Title: Metabolism of benzoquinone ansamycin Hsp90 inhibitors by NQO1

Corresponding Author:

David Ross
Department of Pharmaceutical Sciences, School of Pharmacy,
University of Colorado at Denver and Health Sciences Center,
C-238
4200 East 9th Ave, Denver, CO 80262 USA
e-mail: david.ross@uchsc.edu
Tel: 303-315-3677
Fax: 303-315-6281

The number of Text Pages: 18

The number of Tables: 2

The number of Figures: 5 (plus 2 schemes)

The number of References: 45

The number of words in the Abstract: 332

The number of words in the Introduction: 821

The number of words in the Discussion: 958

Abbreviations

CVFF, consistent valence forcefield; MTT, PDB, Protein Data Bank; RCSB, Research Collaboratory for Structural Bioinformatics.

Molecular Pharmacology Fast Forward. Published on July 6, 2006 as DOI: 10.1124/mol.106.025643
This article has not been copyedited and formatted. The final version may differ from this version.

Abstract

We have previously evaluated the role of NAD(P)H:quinone oxidoreductase 1 (NQO1) in the bioreductive metabolism of 17-(allylamino)-demethoxygeldanamycin (17AAG), to the corresponding hydroquinone, a more potent Hsp90 inhibitor. Here, we report an extensive study with a series of benzoquinone ansamycins, that include geldanamycin, 17-(amino)-17-demethoxygeldanamycin, 17-(allylamino)-17-demethoxygeldanamycin and 17-demthoxy-17-[[2-(dimethylamino)ethyl]amino]-geldanamycin. The reduction of these benzoquinone ansamycins by recombinant human NQO1 to the corresponding hydroquinone ansamycins was monitored by HPLC and confirmed by LC-MS. Inhibition of purified yeast Hsp90 ATPase activity was augmented in the presence of NQO1 and abrogated by 5-methoxy-1,2-dimethyl-3-[(4-nitrophenoxy)methyl]indole-4,7-dione (ES936), a mechanism-based inhibitor of NQO1, demonstrating that the hydroquinone ansamycins were more potent Hsp90 inhibitors than their parent quinones. An isogenic pair of human breast cancer cell lines, MDA468 and MDA468/NQ16, differing in expression of NQO1, were utilized and HPLC analysis demonstrated that hydroquinone ansamycins were formed by the MDA468/NQ16 cells, which could be prevented by ES936 pre-treatment. The MDA468/NQ16 cells were more sensitive to growth inhibition following treatment with the benzoquinone ansamycins, compared to the MDA468 cells; this increased sensitivity could be reduced by ES936 pre-treatment. The increased duration of benzoquinone ansamycin exposure demonstrated increased potency and fold inhibition in MDA468/NQ16 cells relative to the parental MDA468 cells. Computational-based molecular modeling studies displayed additional contacts between yeast Hsp90 and the hydroquinone ansamycins, which translated to greater interaction energies when compared to the corresponding benzoquinone ansamycins. In conclusion, these studies demonstrate that the reduction of this series of benzoquinone ansamycins by NQO1 generates the corresponding hydroquinone ansamycins which exhibit enhanced Hsp90 inhibition.

Molecular Pharmacology Fast Forward. Published on July 6, 2006 as DOI: 10.1124/mol.106.025643
This article has not been copyedited and formatted. The final version may differ from this version.

Introduction

The 90-kDa heat shock protein, Hsp90, is a molecular chaperone responsible for the ATP-dependent folding, stability and function of a number of "client" proteins that are involved in the development and progression of cancer (Isaacs et al., 2003; Maloney and Workman, 2002), these proteins include ErbB2, Raf-1, Cdk4, Met, mutant p53, telomerase hTERT, Hif-1α and the estrogen and androgen receptors. The function of Hsp90 has been shown to be dependent on its ability to bind and hydrolyze ATP (Pearl and Prodromou, 2001; Obermann et al., 1998; Panaretou et al., 1998) and competitive inhibition of ATP binding by the natural product geldanamycin (GM), a benzoquinone ansamycin antibiotic isolated from *Streptomyces hygroscopicus*, leads to the degradation of the client proteins by the ubiquitin-proteosome pathway (An et al., 1997; Schulte et al., 1995; Whitesell et al., 1994), resulting in cell cycle arrest, differentiation and apoptosis (Munster et al., 2001; Hostein et al., 2001). Hsp90 is therefore an attractive cancer drug target in that it has the potential for simultaneous disruption of multiple oncogenic signaling proteins (Goetz et al., 2003; Richter and Buchner, 2001; Adams and Elliott, 2000; Csermely et al., 1998). Furthermore, studies have revealed that the benzoquinone ansamycin Hsp90 inhibitors accumulate in tumour cells more efficiently than in normal tissue leading to high differential selectivities (Chiosis et al., 2003). In addition, immunoprecipitaion studies have demonstrated that Hsp90 from tumour cells has an enhanced affinity for N-terminal ligands, resulting in increased ATPase activity and an increase in sensitivity to benzoquinone ansamycins, than Hsp90 in normal cells (Kamal et al., 2003).

Geldanamycin, the prototypical benzoquinone ansamycin Hsp90 inhibitor, has poor aqueous solubility and displays hepatotoxicity (Supko et al., 1995) and to overcome these undesirable properties a number of geldanamycin analogues of the benzoquinone ansamycin class have been developed, which differ only in their 17-substituent. These include 17-(allylamino)-17-demethoxygeldanamycin (17AAG) which has shown evidence of biological and clinical activity although it has poor solubility and potential toxicity and the more water soluble 17-demthoxy-17-[[2-(dimethylamino)ethyl]amino]-geldanamycin (17DMAG), both are currently in clinical trials (Banerji et al., 2005; Goetz et al., 2005; Smith et al., 2005). The benzoquinone ansamycins are extensively metabolized *in vivo*, the 17-position of 17AAG and 17DMAG is prone to dealkylation by cytochrome P450 to generate the benzoquinone ansamycin and Hsp90 inhibitor 17-(amino)-17-demethoxygeldanamycin (17AG) (Egorin et al., 1998). The redox active quinone moiety, of the benzoquinone ansamycins, is susceptible to reduction by flavin-containing reductases to the semiquinone with subsequent generation of superoxide (Dikalov et al., 2002) or hydroquinone species (Guo et al., 2005; Kelland et al., 1999), which is dependent on one- or two-electron reduction. However, these metabolic pathways could introduce further selectivity to the activation of the benzoquinone ansamycins to a more potent species, the hydroquinone ansamycin, within tumor cells, depending on the levels and type of bioreductive enzyme present.

Molecular Pharmacology Fast Forward. Published on July 6, 2006 as DOI: 10.1124/mol.106.025643
This article has not been copyedited and formatted. The final version may differ from this version.

NAD(P)H:quinone oxidoreductase (EC 1.6.99.2, NQO1, DT-diaphorase) is an obligate two-electron reducing flavin-containing enzyme which can use either NADH or NADPH as reducing cofactors and can catalyze the direct two-electron reduction of quinones to hydroquinones (Ernster 1967). NQO1 is expressed at high levels throughout many human solid tumors and levels are higher in many human tumor cell lines and cancer tissues (colon, stomach, pancreatic, lung and breast) in comparison to the normal equivalents (Cullen et al., 2003; Siegel and Ross, 2000; Siegel et al., 1998). NQO1 has been shown to activate a number of quinone-based bioreductive cytotoxic antitumor agents including diaziquone (AZQ), mitomycin C, 3-[5-aziridinyl-3-(hydroxymethyl)-1-methyl-4,7-dioxoindol-2-yl]prop-2-enol (EO9), streptonigrin, 2,5-diaziridinyl-3-(hydroxylmethyl)-6-methyl-1,4-benzoquinone (RH1), and β-lapachone, by reduction to hydroquinone species (Pink et al., 2000; Winski et al., 1998; Beall et al., 1996; Walton et al., 1991; Siegel et al., 1990a; Siegel et al., 1990b).

The NQO1-mediated reduction of 17AAG using purified NQO1 and the increased sensitivity of human cancer cell lines expressing NQO1 to 17AAG were originally reported by Kelland *et al* (Kelland et al., 1999). We extended these studies to examine the properties of the 17-(allylamino)-17-demethoxygeldanamycin hydroquinone ($17AAGH_2$) formed after reduction of 17AAG by NQO1 (Guo et al., 2005). In addition, we also used the human breast cancer cell line MDA468, deficient in NQO1 due to a genetic polymorphism, and an isogenic paired cell line MDA468/NQ16, a stably transfected clone that expressed high levels of NQO1 protein, in combination with a mechanism-based inhibitor of NQO1 (5-methoxy-1,2-dimethyl-3-[(4-nitrophenoxy)methyl]indole-4,7-dione, (ES936)) to determine the effect of NQO1 on the metabolism of 17AAG in cells. Hsp90 ATPase activity assays with purified yeast and human Hsp90 showed that $17AAGH_2$ was a more potent inhibitor of Hsp90 than the parent quinone (Guo et al., 2005). Molecular modeling studies of 17AAG and $17AAGH_2$ in the nucleotide-binding pocket of the N-terminal domain of the yeast and human Hsp90 crystal structures, displayed a greater number of hydrogen bond interactions with the hydroquinone resulting in greater interaction energies (Guo et al., 2005).

Here, we have examined the reduction of a series of benzoquinone ansamycins, which include GM, 17DMAG, 17AG and 17-demethoxy-17-[[2-(pyrrolidin-1-yl)ethyl]amino]-geldanamycin (17AEP-GA), using purified NQO1 to the corresponding hydroquinone ansamycins (Scheme 1), the inhibition of purified yeast Hsp90 ATPase activity by this series of benzoquinone ansamycins in the presence and absence of NQO1. To confirm the bioreduction of the benzoquinone ansamycins by NQO1 in cells we utilized the human breast cancer cell line MDA468 and the iosgenic paired cell line MDA468/NQO1 in combination with ES936. We have also extended our molecular modeling study to examine the interactions of both the quinone and hydroquinone forms of this series of benzoquinone ansamycins in the N-terminal domain of yeast Hsp90 crystal structure. In this article, we describe the data for this series of benzoquinone ansamycins, where possible we have illustrated the full data set for the series, otherwise we have shown the data for 17DMAG and supplemented the remaining data as supporting information.

Molecular Pharmacology Fast Forward. Published on July 6, 2006 as DOI: 10.1124/mol.106.025643
This article has not been copyedited and formatted. The final version may differ from this version.

Materials and Methods

Materials

Geldanamycin (GM), 17-demethoxy-17-[[2-(dimethylamino)ethyl]amino]-geldanamycin (17DMAG) and 17-demethoxy-17-[[2-(pyrrolidin-1-yl)ethyl]amino]-geldanamycin (17AEP-GA) were obtained from Invivogen Inc (San Diego, CA); 17-(allylamino)-17-demethoxygeldanamycin (17AAG) and 17-(amino)-17-demethoxygeldanamycin (17AG) was provided by the National Cancer Institute and Kosan Biosciences (Hayward, CA). 2,6-Dichlorophenol-indophenol (DCPIP), NADH, NADPH, sodium borohydride, 3-(4,5-dimethylthiazol-2-yl)-2,5-diphenyltetrazolium bromide (MTT), bovine serum albumin (BSA), β-lapachone, N-phenyl-1-naphthylamine, D(-)penicillamine were obtained from the Sigma Chemical Co. (St. Louis MO). Malachite green phosphate assay kit was obtained from BioAssay Systems Inc (Hayward CA). Mouse anti-Hsp70 and rabbit anti-Raf-1 antibodies were obtained from Stressgen (Vancouver, British Columbia, Canada). 5-methoxy-1,2-dimethyl-3-[(4-nitrophenoxy)methyl]indole-4,7-dione (ES936) was supplied by Professor Christopher J. Moody (School of Chemistry, University of Nottingham, Nottingham, United Kingdom). Yeast Hsp90 and radicicol were obtained from Alexis (San Diego, CA). Recombinant human NQO1 (rhNQO1) was purified from *Escherichia coli* as described previously (Beall et al., 1994). The activity of rhNQO1 was 4.5 μmol DCPIP/min/mg protein.

Cell lines

The human breast cancer cell line MDA468 and the NQO1 stably transfected cell line MDA468/NQ16 have been described previously (Dehn et al., 2004). Cells were grown in RPMI 1640 containing 10% (v/v) fetal bovine serum and 1% (v/v) penicillin, streptomycin, and glutamine. MDA468 and MDA468/NQ16 cell sonicates were prepared from by probe sonication in ice-cold 25 mmol/L Tris-HCl (pH 7.4) containing 250 mmol/L sucrose and 5 μmol/L flavin adenine dinucleotide.

Inhibition of NQO1 by ES936

The inhibition of NQO1 by ES936, a potent mechanism-based inhibitor of NQO1, was achieved using a single dose of ES936 100 nmol/L which was nontoxic and resulted in >96% inhibition of NQO1 activity after 4 hours in MDA468/NQ16 cells (Dehn et al., 2003).

HPLC and LC-MS analysis

The metabolism of the benzoquinone ansamycins by NQO1 was analyzed by high performance liquid chromatography (HPLC) on a Luna C18 5μm, 4.6 x 250mm reverse-phase column (Phenomenex, Torrance, CA) at room temperature. HPLC conditions were as follows: buffer A, 50 mmol/L ammonium acetate (pH 4) containing 10 μmol/L D(-)-penicillamine; buffer B, methanol (100%). Both buffers were continuously bubbled with argon, gradient, 30% B to 90% B over 10 minutes and then 90% B for 5 minutes (flow rate of 1 ml/min). The sample

Molecular Pharmacology Fast Forward. Published on July 6, 2006 as DOI: 10.1124/mol.106.025643
This article has not been copyedited and formatted. The final version may differ from this version.

injection volume was 50µl. Liquid Chromatography Mass Spectrometry (LC-MS) was performed using positive ion electrospray ionization and the mass spectra were obtained with a PE Sciex API-3000 triple quadrupole MS (Foster City, CA) with a turbo ion spray source interfaced to a PE Sciex 200 HPLC system. Samples were chromatographed on a Luna C18 5µm, 50 x 2mm reverse-phase column (Phenomenex, Torrance, CA) using a gradient elution consisting of a 2 minute initial hold at 20% B followed by an increase to 80% B over 20 minutes at a flow rate of 200 µl/min and a sample injection volume of 20 µL. Solvent A, 10 mmol/L ammonium acetate containing 0.1% (v/v) acetic acid (pH 4.4) and solvent B, 10 mmol/L ammonium acetate in acetonitrile containing 0.1% (v/v) acetic acid. The mass spectrometer settings were turbo ion spray temperature of 250ºC, spray needle voltage at 4,500V, declustering potential at 35V, and focus plate at 125V. Mass spectra were continuously recorded from 150 to 1000 amu every 3 seconds during the chromatographic analysis.

Hsp90 ATPase activity assay

Inhibition of yeast Hsp90 ATPase was measured as described previously (Rowlands et al., 2004). In brief, 2.5µg of purified yeast Hsp90 was incubated in 100 mmol/L Tris-HCl (pH 7.4) containing 20 mmol/L KCl, 6 mmol/L $MgCl_2$, 200 µmol/L NADH, the appropriate benzoquinone ansamycin (2 µmol/L and 4 µmol/L) with or without 0.33µg rhNQO1, and 2 µmol/L ES936. Reactions (25µL) were started by the addition of 1 mmol/L ATP and allowed to proceed at 37ºC for 3 hours. Reactions were then diluted with 225µL of 100 mmol/L Tris-HCl (pH 7.4) containing 20 mmol/L KCl and 6 mmol/L $MgCl_2$ mixed thoroughly, and 80µL were transferred to each well (96-well plate) followed by 20µL malachite green reagent. After 10 minutes, trisodium citrate (83 mmol/L) was added to stabilize the color and plates were read at 650 nm.

Growth inhibition assays

Growth inhibition was measured using the MTT assay. Cells were seeded at 2 x 10^3 per well (96-well plate) in complete medium for 16 hours. The cells were then pretreated with 100 nmol/L ES936 or an equal amount of DMSO for 30 minutes and then exposed to the appropriate benzoquinone ansamycin for 4 hours, after which cells were washed free of drug and incubated in fresh medium for an additional 72 hours. The increase in drug exposure time from 4 hours to 72 hours (continuous exposure) was performed for 17AAG and 17DMAG. Cell viability was measured by the MTT assay as described previously (Winski et al., 2001). Inhibition of rhNQO1 by ES936 was >98%.

Immunoblot analysis

MDA468 and MDA468/NQ16 cells were grown in 100-mm plates in complete medium to ~70% confluency. For Hsp70 and Raf-1 analysis, cells were treated with DMSO or 17DMAG (50-100 nmol/L) in 10 mL complete medium for 24 hours. Following drug treatment, cells were washed in PBS and then lysed by the addition of radioimmunoprecipitation assay buffer [50 mmol/L Tris-HCl (pH 7.4), 0.5% (v/v) NP40] containing 1 Mini protease tablet (protease inhibitor cocktail, Roche, Indianapolis, IN) and phosphatase inhibitors (30 mmol/L NaF,

Molecular Pharmacology Fast Forward. Published on July 6, 2006 as DOI: 10.1124/mol.106.025643
This article has not been copyedited and formatted. The final version may differ from this version.

40 mmol/L β-glycerophosphate, 20 mmol/L sodium pyrophosphate, 1 mmol/L orthovanadate, 1 mmol/L EGTA). Lysates were probe sonicated (2 seconds) on ice and then centrifuged to remove cellular debris. Protein concentrations were determined on supernatant by the method of Lowry *et al*. (Lowry et al., 1951). Samples were heated to 70ºC in 2 x Laemmli SDS sample buffer, and proteins were separated by 12% SDS-PAGE (precast minigel, Bio-Rad, Hercules CA) and then transferred to 0.4-µm polyvinylidene difluoride membranes. Membranes were blocked in 10 mmol/L Tris-HCl (pH 8.0), 150 mmol/L NaCl, 0.2% Tween 20, and 5% nonfat milk for a minimum of 1 hour at room temperature. Anti-Hsp70 and anti-Raf antibodies were added for 1 hour at room temperature. All primary antibodies were diluted 1:1,000m except actin (1:5,000). Horseradish peroxidase-labeled secondary antibodies (Jackson ImmunoResearch Labs, West Grove, PA) were diluted 1:5,000 and added for 30 minutes. Proteins were visualized using enhanced chemiluminescence detection.

Molecular modeling of the benzoquinone ansamycin and corresponding hydroquinone ansamycin in the amino-terminal domain of the yeast Hsp90 crystal structure

Molecular modeling studies were performed on a Silicon Graphics Octane 2 workstation using the InsightII software package version 2000 (Accelrys, Inc., San Diego, CA). The crystallographic coordinates for the 2.5Å structure of the amino-terminal domain of yeast Hsp90, PDB: 1A4H (Prodromou et al., 1997) were obtained from the RCSB Protein Data Bank. The Builder Module was used to add hydrogens to the protein structure and the ionizable residues were corrected for physiologic pH. The benzoquinone ansamycin and the corresponding hydroquinone structures were constructed and assigned the correct atom type and bond order, from the co-crystallized geldanamycin structure. Once constructed, the ligands were in turn positioned, using the coordinated system of the protein, in the nucleotide-binding domain of Hsp90, the ligand assembly was then associated with the Hsp90 protein structure. For the molecular mechanics and molecular dynamics calculations, the Discover Module was used and the potentials and charges of the Hsp90-ligand complex were corrected using CVFF (Dauber-Osguthorpe et al., 1988). The Hsp90-ligand complex was then minimized using the conjugate gradient method (1,000 iterations). The Docking Module was used to perform the intermolecular energy calculation to determine the non-bonded interaction energy between the Hsp90 protein and the appropriate ligand. An interface 6Å radius subset encompassing the ligand-binding domain was selected and both van der Waals and electrostatic energies were calculated with a specified cutoff of 8Å.

Molecular Pharmacology Fast Forward. Published on July 6, 2006 as DOI: 10.1124/mol.106.025643
This article has not been copyedited and formatted. The final version may differ from this version.

Results

The reduction of this benzoquinone ansamycin series using purified rhNQO1, with either NADH or NADPH as cofactors, generated the corresponding hydroquinone ansamycin. The incubation of the benzoquinone ansamycin of interest with rhNQO1 and NADH, was monitored by HPLC analysis, resulted in the generation of the polar hydroquinone ansamycin metabolite with subsequent loss of the benzoquinone ansamycin (Figure 1A and B data shown for 17DMAG for other compounds see supplemental data). The formation of the hydroquinone ansamycin, from the corresponding benzoquinone ansamycin, was NQO1 dependent and could be prevented by ES936, a mechanism-based inhibitor of NQO1 (Figure 1C data shown for 17DMAG for other compounds see supplemental data). In addition, the benzoquinone ansamycins could be chemically reduced using sodium borohydride to generate the hydroquinone ansamycin as previously reported (Guo et al., 2005, Schnur et al., 1995). The identification of the hydroquinone ansamycin product, from the chemical or NQO1-mediated reduction of the benzoquinone ansamycin, was confirmed by LC-MS giving ions for GMH_2 at *m/z* 580.5 $[M+NH_4^+]^+$, $17AGH_2$ at *m/z* 548.2 $[M+H^+]^+$, $17DMAGH_2$ at *m/z* 619.3 $[M+H^+]^+$ and $17AEP\text{-}GAH_2$ at *m/z* 645.3 $[M+H^+]^+$ (Figure 1 D data shown for 17DMAG for other compounds see supplemental data). All of the hydroquinone ansamycins formed by the reduction of the benzoquinone ansamycins in this series were susceptible to autooxidation. The rate of autooxidation of the hydroquinone ansamycin was dependent on the substituent at the 17-position, from our studies, the geldanamycin hydroquinone from this series was the most stable (data not shown). The autooxidation of the hydroquinone ansamycin could be impeded by continuously gassing the HPLC buffers during analysis with nitrogen or argon and by the addition of a copper chelator to the HPLC buffers (see Materials and Methods).

The malachite green Hsp90 ATPase activity assay, has been previously utilized as a high-throughput screen to evaluate Hsp90 inhibition (Rowlands et al., 2004), it was employed here to examine the differences in inhibitory activity of this series of benzoquinone ansamycins and their respective hydroquinones on the yeast Hsp90 ATPase reaction (Figure 2). In these assays, purified yeast Hsp90 and ATP was incubated with the appropriate benzoquinone ansamycin (2μM and 4μM) and NADH in the presence and absence of rhNQO1, over a 3 hour time period, after which reactions were terminated and the concentration of inorganic phosphate was measured using the malachite green assay (Rowlands et al., 2004). A significant decrease in ATPase activity was observed with each of the benzoquinone ansamycins examined in the presence of NQO1, in comparison to that obtained for the benzoquinone ansamycins with NADH, and this could be prevented by pre-treatment with ES936. At these concentrations minimal inhibition of the Hsp90-mediated ATPase reaction was observed for 17DMAG and 17AEP-GA, which further highlighted the effect of the hydroquinone ansamycin on Hsp90 inhibition. The results from this ATPase assay showed that for this series of benzoquinone ansamycins, the hydroquinone ansamycin, generated by NQO1, was the more potent Hsp90 inhibitor.

Molecular Pharmacology Fast Forward. Published on July 6, 2006 as DOI: 10.1124/mol.106.025643
This article has not been copyedited and formatted. The final version may differ from this version.

These studies were extended to a cell-based system and the formation of the hydroquinone ansamycins was investigated in cell sonicates prepared from the isogenic MDA468 and MDA468/NQ16 human breast cancer cell lines. These cell lines have been used previously to examine the role of NQO1 in antitumor quinone metabolism (Dehn et al., 2004), including 17AAG (Guo et al., 2005). The parental MDA468 cell line is deficient in NQO1 (<10 nmol DCPIP/min/mg) because of homozygous expression of the NQO1*2 polymorphism (Traver et al., 1997). The MDA468/NQ16 cell line was generated by the stable transfection of the parental MDA468 cell line with human NQO1, resulting in high NQO1 activity (>1,800 nmol DCPIP/min/mg). The HPLC analysis of MDA468 and MDA468/NQ16 cell sonicates treated with these benzoquinone ansamycins yielded similar results to those obtained previously with 17AAG (Guo et al., 2005). The hydroquinone ansamycins were not detected in the MDA468 cell sonicates (Figure 3A data shown for 17DMAG for other compounds see supplemental data). Whereas, the MDA468/NQ16 cell sonicates readily generated the hydroquinone ansamycin (Figure 3B data shown for 17DMAG for other compounds see supplemental data), which was NADH or NADPH dependent and the formation of the hydroquinone could be prevented by ES936 (Figure 3C data shown for 17DMAG for other compounds see supplemental data).

The effect of growth inhibition induced by this series of benzoquinone ansamycins in the MDA468 and MDA468/NQ16 cells was determined by MTT assay. In this study, the cells were treated with the benzoquinone ansamycin for 4 hours in the presence and absence of ES936 (Figure 4A and B data shown for 17DMAG for other compounds see supplemental data). The results from these experiments showed that MDA468/NQ16 cells had increased sensitivity to the benzoquinone ansamycin (17DMAG; IC_{50}, 0.22 ± 0.05 μmol/L) compared with parental MDA468 cells (17DMAG; IC_{50}, 2.06 ± 0.25 μmol/L). The sensitivity to the benzoquinone ansamycin could be abrogated by pre-treatment with ES936 (17DMAG + ES936; IC_{50}, 1.81 ± 0.20 μmol/L). The natural product, non-quinone Hsp90 inhibitor, radicicol, was used as a negative control and the growth-inhibitory effects were essentially identical in MDA468 and MDA468/NQ16 cells, reinforcing the effect of the hydroquinone on the growth inhibition observed in MDA468/NQ16 cells (Table 1). In addition, the effect of 17AAG and 17DMAG exposure time on the MDA468/NQ16 cells and the MDA468 cells was examined using the MTT cytotoxicity assay. The fold increase in growth inhibition in MDA468/NQ16 cells relative to MDA468 cells was 12 fold with 17AAG and 9 fold with 17DMAG after a 4 hour exposure. An increase in the time of exposure of cells to 17AAG or 17DMAG from 4 hours to 72 hours, resulted in the increase of fold potentiation in MDA468/NQ16 cells relative to MDA468 cells to 66 fold with 17AAG (Figure 4C) and 15 fold with 17DMAG (Figure 4D) respectively. In agreement with cellular data, the potentiated inhibition of Hsp90 observed in MDA468/NQ16 cells resulted in increased degradation of the Hsp90 client protein, Raf-1, with a corresponding increase in Hsp70 induction (Figure 4E data shown for 17DMAG) relative to the parental MDA468 cells.

Molecular modeling studies of this series of benzoquinone ansamycins and their corresponding hydroquinones into the ATP-binding site of the yeast Hsp90 crystal structure revealed significant differences in the binding energies

Molecular Pharmacology Fast Forward. Published on July 6, 2006 as DOI: 10.1124/mol.106.025643
This article has not been copyedited and formatted. The final version may differ from this version.

post-minimization. The non-bonded interaction energy is the sum of the van der Waals and electrostatic energies, the measure of the affinity between the Hsp90 protein and the ligand investigated. In all the benzoquinone ansamycins examined, the hydroquinone had a greater non-bonded interaction energy than the parent quinone. These data support the hypothesis that the hydroquinone ansamycin is a more potent inhibitor of Hsp90. Following minimization, the Hsp90-ligand complex was visualized to identify important amino acid residues in the ATP-binding domain that interact *via* hydrogen bonding with the ligand investigated; there was no significant change in the global conformation of Hsp90. A number of protein-ligand and through-solvent interactions lock the macrocycle of benzoquinone and the hydroquinone ansamycins in an overall conformation similar to that reported for the original yeast Hsp90-geldanamycin co-crystallized structure (Prodromou et al., 1997). The Hsp90-hydroquinone ansamycin complex revealed additional direct hydrogen-bonding interactions between the hydroquinone ansamycin and the Hsp90 protein, accounting for the greater interaction energy (Table 2 data shown for 17DMAG for other compounds see supplemental data), compared to the parent quinone. In the ATP-binding domain of yeast Hsp90, the C21 ketone of the benzoquinone ansamycins hydrogen bonds with the amine of Lys98 and the C18 ketone of the quinone ring system interacts with a water molecule that in turn contacts Asp40 (Figure 5A and C data shown for 17DMAG for other compounds see supplemental data). The C21 hydroxyl of the hydroquinone ansamycins GMH_2, $17AGH_2$ and $17AEP\text{-}GAH_2$ also hydrogen bonds with the amine of Lys98 and the C18 hydroxyl of the hydroquinone ring system directly hydrogen bonds to Asp40, whereas the C21 hydroxyl of $17AAGH_2$ and $17DMAG_2$ does not interact directly with Lys98. The hydrogen atom of the C18 hydroxyl, in all of the hydroquinone ansamycins examined, interacts with an oxygen atom of the carboxylate side chain of Asp40, which results in a more compact C-clamp conformation around helix-2 and in the case of the 17-amino-substituted ansamycins the hydroquinone allows the amide of the ansa ring to interact with the backbone nitrogen of Phe124 (Figure 5B and D data shown for 17DMAG for other compounds see supplemental data). Although no direct interactions were observed with yeast Hsp90 and the 17-substituent of the benzoquinone ansamycins or their respective hydroquinones, the side chain is orientated into solvent and does not appear to directly interfere with the binding of the ligands to the Hsp90 binding pocket.

Molecular Pharmacology Fast Forward. Published on July 6, 2006 as DOI: 10.1124/mol.106.025643
This article has not been copyedited and formatted. The final version may differ from this version.

Discussion

The reduction of 17AAG by NQO1 and the correlation between the cellular levels of NQO1 and sensitivity to 17AAG, was first reported by Kelland *et al* (Kelland et al., 1999). They also described increased inhibitory activity of geldanamycin and 17AAG in NQO1-transfected BE cells relative to NQO1-null BE parental cells and suggested that NQO1 may play a role in the cellular metabolism of these benzoquinone ansamycins (Kelland et al., 1999). We extended these studies for 17AAG by examining the purified rhNQO1-mediated reduction of 17AAG; identification of the reduction product, $17AAGH_2$, by HPLC and LC-MS; assessing the inhibition of Hsp90 ATPase activity of 17AAG and $17AAGH_2$ generated by NQO1 and abrogated by ES936; examining toxicity in isogenic MDA468 and MDA468/NQ16 cells and investigating the interactions of 17AAG and $17AAGH_2$ in the ATP binding domain of Hsp90 by computational modeling (Guo et al., 2005).

In this article, we have examined a series of benzoquinone anamycins, differing in structure only at the 17-position, to determine whether the "active" hydroquinone ansamycin hypothesis can be applied to a range of the common benzoquinone ansamycin compounds, including 17DMAG which is currently in phase I trials in patients with metastatic, unresectable solid tumors and lymphomas. In each case we achieved reduction of the benzoquinone ansamycin to the corresponding hydroquinone ansamycin using purified rhNQO1, the resulting hydroquinone was identified by HPLC and LC-MS. To confirm that the hydroquinone ansamycins, generated by NQO1, were more potent Hsp90 inhibitors than their respective parent quinones, we used purified yeast Hsp90 to assess the ATPase activity. Indeed as expected, the hydroquinone ansamycins were more potent inhibitors of the yeast Hsp90 ATPase reaction. The inhibition of ATPase activity by the hydroquinone ansamycins could be abrogated by use of ES936, a mechanism-based inhibitor of NQO1, confirming the role of the hydroquinone moiety in potentiating Hsp90 inhibition.

The NQO1-dependent formation of the hydroquinone ansamycins was detected by HPLC analysis in MDA468/NQ16 sonicates but not in MDA468 sonicates and could be blocked by use of ES936. Furthermore, the effect of this series of benzoquinone ansamycins on growth inhibition was increased in MDA468/NQ16 cells relative to the NQO1-deficient parental MDA468 cell line, which was consistent with previous data (Guo et al., 2005, Kelland et al., 1999). The inhibition of NQO1 with ES936 in MDA468/NQ16 cells resulted in growth inhibitory activity of the benzoquinone ansamycins to approximately those observed in the parental MDA468 cells. In addition, the non-quinone Hsp90 inhibitor, radicicol, displayed essentially the same growth inhibitory profile in both MDA468 and MDA468/NQ16 cells. These data clearly demonstrate that the increased sensitivity in cells containing elevated NQO1 levels is due to the reduction of the benzoquinone ansamycin to the more active hydroquinone form and in concurrence with previous data (Guo et al., 2005). The increased fold potentiation of 17AAG and 17DMAG in MDA468/NQ16 relative to MDA468 cells with increased exposure time may be a result of increased accumulation of the hydroquinone ansamycin, generated by NQO1, in cells over time, due to the

Molecular Pharmacology Fast Forward. Published on July 6, 2006 as DOI: 10.1124/mol.106.025643
This article has not been copyedited and formatted. The final version may differ from this version.

decreased lipid solubility of the hydroquinone form relative to the parent quinone. The differences in fold potentiation between 17AAG and 17DMAG could be due to the rate of NQO1-mediated reduction, as 17AAG is reduced at a faster rate relative to 17DMAG (data not shown), or the stability of the hydroquinone ansamycin formed. Therefore, the marked increase in fold potentiation, particularly with 17AAG, could be significant with respect to anti-tumor effect, in tumors containing high levels of NQO1. The amount of NQO1 needed to generate adequate levels of hydroquinone ansamycin sufficient for optimal growth inhibitory activity will vary from cell to cell and will depend on a variety of factors including the reduction rate, the stability of the hydroquinone generated and the rate of repair of any cellular damage resulting from Hsp90 inhibition.

Computational-based modeling studies of the benzoquinone ansamycins and the hydroquinone ansamycins in the nucleotide-binding domain, of the N-terminal domain, of the yeast Hsp90 crystal structure, displayed a greater number of hydrogen bond interactions between the Hsp90 protein and the hydroquinone ansamycin, resulting in increased total interaction energies compared to the parent quinone. The benzoquinone ansamycin and hydroquinone ansamycin series investigated in this study differed only in substitution at the 17-position, and in all instances the 17-substituent pointed into solvent and did not appear to interact directly with the Hsp90 protein. The greater interaction energies of the hydroquinone ansamycins can be explained by the additional direct hydrogen bond contacts with the Hsp90 protein, mainly due to the hydrogen bond donor contribution of the hydroquinone moiety, which results in a more compact C-shaped conformation which is evident from the hydrogen bonding interaction between the C18 hydroxyl and the Asp40 residue of helix-2, the strength of this interaction, as indicated by the hydrogen bond length, appears to correlate with the electrostatic contribution to the non-bonded interaction energy across this hydroquinone ansamycin series. The more compact conformation of the hydroquinone ansamycin around helix-2, the greater protein-hydroquinone ansamycin hydrogen bond contacts and the resultant greater interaction energies for the hydroquinone ansamycins relative to the parent quinone for this series provide explanation as to why the hydroquinone ansamycins are more potent Hsp90 inhibitors.

In summary, our data show that for this series of benzoquinone ansamycins, the hydroquinone can be generated more efficiently in tumor cells containing high levels of NQO1 and that the hydroquinone form, based upon target inhibition in both cell-free, cellular systems and molecular modeling studies, represents a more potent inhibitor of Hsp90. Although the parent benzoquinone ansamycins retain the ability to inhibit Hsp90 in a concentration dependent manner, the superior Hsp90 inhibitory potency of he hydroquinone ansamycins relative to their parent quinones has important implications for drug development.

A rational extension to this research would be to develop a prodrug approach (Scheme 2), to deliver the more potent hydroquinone ansamycin intracellularly. The generation of a series of hydroquinone ansamycin prodrugs would initially circumvent the NQO1-mediated reduction of the benzoquinone ansamycin and may additionally improve the solubility and bioavailability characteristics of the Hsp90 inhibitor. An ideal prodrug candidate would

Molecular Pharmacology Fast Forward. Published on July 6, 2006 as DOI: 10.1124/mol.106.025643
This article has not been copyedited and formatted. The final version may differ from this version.

generate, via intracellular enzymatic hydrolysis, a relatively stable hydroquinone ansamycin, which is also a potent inhibitor of Hsp90 and in its quinone form is a good substrate for NQO1 to facilitate reduction back to the more potent Hsp90 inhibitor, the hydroquinone ansamycin. In addition, the hydroquinone ansamycin has increased water solubility and a decreased tendancy to cross cell membranes leading to increased accumulation of the more potent Hsp90 inhibitor, the hydroquinone ansamycin, in tumor cells containing NQO1 (Guo et al., 2005, Workman 2003). This prodrug approach may further improve the selectivity of the Hsp90 inhibitor, in that the hydrolyzing enzyme may be specific to or more abundant in a certain tissue type.

Molecular Pharmacology Fast Forward. Published on July 6, 2006 as DOI: 10.1124/mol.106.025643
This article has not been copyedited and formatted. The final version may differ from this version.

References

Adams J, Elliott PJ. (2000) New agents in cancer clinical trials. *Oncogene* **19**:6687-92.

An WG, Schnur RC, Neckers L, Blagosklonny MV. (1997) Depletion of p185erbB2, Raf-1 and mutant p53 proteins by geldanamycin derivatives correlates with antiproliferative activity. *Cancer Chemother Pharmacol* **40**:60-4.

Banerji U, Walton M, Raynaud F, Grimshaw R, Kelland L, Valenti M, Judson I, Workman P. (2005) Pharmacokinetic-pharmacodynamic relationships for the heat shock protein 90 molecular chaperone inhibitor 17-allylamino, 17-demethoxygeldanamycin in human ovarian cancer xenograft models. *Clin Cancer Res* **11**:7023-32.

Beall HD, Liu Y, Siegel D, Bolton EM, Gibson NW, Ross D. (1996) Role of NAD(P)H:quinone oxidoreductase (DTdiaphorase) in cytotoxicity and induction of DNA damage by streptonigrin. *Biochem Pharmacol* **51**: 645-52.

Beall HD, Mulcahy RT, Siegel D, Traver RD, Gibson NW, Ross D. (1994) Metabolism of bioreductive antitumor compounds by purified rat and human DT-diaphorases. *Cancer Res* **54**:3196-201.

Chiosis G, Huezo H, Rosen N, Mimnaugh E, Whitesell L, Neckers L. (2003) 17AAG: low target binding affinity and potent cell activity-finding an explanation. *Mol Cancer Ther* **2**:123-9.

Csermely P, Schnaider T, Soti C, Prohaszka Z, Nardai G. (1998) The 90-kDa molecular chaperone family: structure, function, and clinical applications. A comprehensive review. *Pharmacol Ther* **79**:129-68.

Cullen JJ, Hinkhouse MM, Grady M, Gaut AW, Liu J, Zhang YP, Weydert CJ, Domann FE, Oberley LW. (2003) Dicumarol inhibition of NADPH:quinone oxidoreductase induces growth inhibition of pancreatic cancer via a superoxide mediated mechanism. *Cancer Res* **63**:5513-20.

Dauber-Osguthorpe P, Roberts VA, Osguthorpe DJ, Wolff J, Genest M, Hagler AT. (1988) Structure and energetics of ligand binding to proteins: *Escherichia coli* dihydrofolate reductase-trimethoprim, a drug-receptor system. *Proteins* **4**:31-47.

Dehn DL, Siegel D, Swann E, Moody CJ, Ross D. (2003) Biochemical, cytotoxic and genotoxic effects of ES936, a mechanism-based inhibitor of NAD(P)H:quinone oxidoreductase 1 in cellular systems. *Mol Pharmacol* **64**:714-720.

Dehn DL, Winski SL, Ross D. (2004) Development of a new isogenic cell-xenograft system for evaluation of NAD(P)H:quinone oxidoreductase-directed antitumor quinones: evaluation of the activity of RH1. *Clin Cancer Res* **10**:3147-55.

Dikalov S, Landmesser U, Harrison DG. (2002) Geldanamycin leads to superoxide formation by enzymatic and non-enzymatic redox cycling. Implications for studies of Hsp90 and endothelial cell nitric-oxide synthase. *J Biol Chem* **277**:25480-5.

Egorin MJ, Rosen DM, Wolff JH, Callery PS, Musser SM, Eiseman JL. (1998) Metabolism of 17-(allylamino)-17-demethoxygeldanamycin (NSC 330507) by murine and human hepatic preparations. *Cancer Res* **58**:2385-96.

Ernster L. (1967) DT-diaphorase. *Methods Enzymol* **10**:309-17.

Goetz MP, Toft D, Reid J, Ames M, Stensgard B, Safgren S, Adjei AA, Sloan J, Atherton P, Vasile V, Salazaar S, Adjei A, Croghan G, Erlichman C. (2005) Phase I trial of 17-allylamino-17-demethoxygeldanamycin in patients with advanced cancer. *J Clin Oncol* **23**:1078-87.

Goetz MP, Toft DO, Ames MM, Erlichman C. (2003) The Hsp90 chaperone complex as a novel target for cancer therapy. *Ann Oncol* **14**:1169-76.

Guo W, Reigan P, Siegel D, Zirrolli J, Gustafson D, Ross D. (2005) Formation of 17-allylamino-demethoxygeldanamycin (17-AAG) hydroquinone by NAD(P)H:quinone oxidoreductase 1: role of 17-AAG hydroquinone in heat shock protein 90 inhibition. *Cancer Res* **65**:10006-15.

Hostein I, Robertson D, DiStefano F, Workman P, Clarke PA. (2001) Inhibition of signal transduction by the Hsp90 inhibitor 17-allylamino-17-demethoxygeldanamycin results in cytostasis and apoptosis. *Cancer Res* **61**:4003-9.

Isaacs JS, Xu W, Neckers L. (2003) Heat shock protein 90 as a molecular target for cancer therapeutics. *Cancer Cell* **3**:213-7.

Kamal A, Thao L, Sensintaffar J, Zhang L, Boehm MF, Fritz LC, Burrows FJ. (2003) A high-affinity conformation of Hsp90 confers tumour selectivity on Hsp90 inhibitors. *Nature* **425**:407-10.

Kelland LR, Sharp SY, Rogers PM, Myers TG, Workman P. (1999) DT-Diaphorase expression and tumor cell sensitivity to 17-allylamino-17-demethoxygeldanamycin, an inhibitor of heat shock protein 90. *J Natl Cancer Inst* **91**:1940-9.

Lowry OH, Rosebrough NJ, Farr AL, Randall RJ. (1951) Protein measurement with the Folin phenol reagent. *J Biol Chem* **193**:265-75.

Maloney A, Workman P. (2002) HSP90 as a new therapeutic target for cancer therapy: the story unfolds. *Expert Opin Biol Ther* **2**:3-24.

Munster PN, Srethapakdi M, Moasser MM, Rosen N. (2001) Inhibition of heat shock protein 90 function by ansamycins causes the morphological and functional differentiation of breast cancer cells. *Cancer Res* **61**:2945-52.

Obermann WM, Sondermann H, Russo AA, Pavletich NP, Hartl FU. (1998) In vivo function of Hsp90 is dependent on ATP binding and ATP hydrolysis. *J Cell Biol* **143**:901-10.

Panaretou B, Prodromou C, Roe SM, O'Brien R, Ladbury JE, Piper PW, Pearl LH. (1998) ATP binding and hydrolysis are essential to the function of the Hsp90 molecular chaperone in vivo. *EMBO J* **17**:4829-36.

Pearl LH, Prodromou C. (2001) Structure, function, and mechanism of the Hsp90 molecular chaperone. *Adv Protein Chem* **59**:157-86.

Pink JJ, Planchon SM, Tagliarino C, Varnes ME, Siegel D, Boothman DA. (2000) NAD(P)H:quinone oxidoreductase activity is the principal determinant of β-lapachone cytotoxicity. *J Biol Chem* **275**:5416-24.

Prodromou C, Roe SM, O'Brien R, Ladbury JE, Piper PW, Pearl LH. (1997) Identification and structural characterization of the ATP/ADP-binding site in the Hsp90 molecular chaperone. *Cell* **90**:65-75.

Richter K, Buchner J. (2001) Hsp90: chaperoning signal transduction. *J Cell Physiol* **188**:281-90.

Rowlands MG, Newbatt YM, Prodromou C, Pearl LH, Workman P, Aherne W. (2004) High-throughput screening assay for inhibitors of heat-shock protein 90 ATPase activity. *Anal Biochem* **327**:176-83.

Schnur RC, Corman ML, Gallaschun RJ, Cooper BA, Dee MF, Doty JL, Muzzi ML, Moyer JD, DiOrio CI, Barbacci EG, Miller PE, O'Brien AT, Morin MJ, Foster BA, Pollack VA, Savage DM, Sloan DE, Pustilnik LR,

and Moyer MP. (1995) Inhibition of the oncogene product p185erbB-2 in vitro and in vivo by geldanamycin and dihydrogeldanamycin derivatives. *J Med Chem* **38**:3806-12.

Schulte TW, Blagosklonny MV, Ingui C, Neckers L. (1995) Disruption of the Raf-1-Hsp90 molecular complex results in destabilization of Raf-1 and loss of Raf-1-Ras association. *J Biol Chem* **270**:24585-8.

Siegel D, Franklin WA, Ross D. (1998) Immunohistochemical detection of NAD(P)H:quinone oxidoreductase in human lung and lung tumors. *Clin Cancer Res* **4**:2065-70.

Siegel D, Gibson NW, Preusch PC, Ross D. (1990a) Metabolism of mitomycin C by DT-diaphorase: role in mitomycin C-induced DNA damage and cytotoxicity in human colon carcinoma cells. *Cancer Res* **50**:7483-9.

Siegel D, Gibson NW, Preusch PC, Ross D. (1990b) Metabolism of diaziquone by NAD(P)H:(quinone acceptor) oxidoreductase (DT-diaphorase): role in diaziquone induced DNA damage and cytotoxicity in human colon carcinoma cells. *Cancer Res* **50**:7293-300.

Siegel D, Ross D. (2000) Immunodetection of NAD(P)H:quinone oxidoreductase 1 (NQO1) in human tissues. *Free Radic Biol Med* **29**:246-53.

Smith V, Sausville EA, Camalier RF, Fiebig HH, Burger AM. (2005) Comparison of 17-dimethylaminoethylamino-17-demethoxy-geldanamycin (17DMAG) and 17-allylamino-17-demethoxygeldanamycin (17AAG) in vitro: effects on Hsp90 and client proteins in melanoma models. *Cancer Chemother Pharmacol* **56**:126-37.

Supko JG, Hickman RL, Grever MR, Malspeis L. (1995) Preclinical pharmacologic evaluation of geldanamycin as an antitumor agent. *Cancer Chemother Pharmacol* **36**:305-15.

Traver RD, Siegel D, Beall HD, Phillips RM, Gibson NW, Franklin WA, Ross D. (1997) Characterization of a polymorphism in NAD(P)H: quinone oxidoreductase (DT-diaphorase). *Br J Cancer* **75**:69-75.

Walton MI, Smith PJ, Workman P. (1991) The role of NAD(P)H:quinone reductase (EC 1.6.99.2, DT-diaphorase) in the reductive bioactivation of the novel indoloquinone antitumor agent EO9. *Cancer Commun* **3**:199-206.

Whitesell L, Mimnaugh EG, De Costa B, Myers CE, Neckers LM. (1994) Inhibition of heat shock protein HSP90-pp60v-src heteroprotein complex formation by benzoquinone ansamycins: essential role for stress proteins in oncogenic transformation. *Proc Natl Acad Sci USA* **91**:8324-8.

Winski SL, Hargreaves RH, Butler J, Ross D. (1998) A new screening system for NAD(P)H:quinone oxidoreductase (NQO1)-directed antitumor quinones: identification of a new aziridinylbenzoquinone, RH1, as a NQO1-directed antitumor agent. *Clin Cancer Res* **4**:3083-8.

Winski SL, Swann E, Hargreaves RH, Dehn DL, Butler J, Moody CJ, Ross D. (2001) Relationship between NAD(P)H:quinone oxidoreductase 1 (NQO1) levels in a series of stably transfected cell lines and susceptibility to antitumor quinones. *Biochem Pharmacol* **61**:1509-16.

Workman P. (2003) Auditing the pharmacological accounts for Hsp90 molecular chaperone inhibitors: unfolding the relationship between pharmacokinetics and pharmacodynamics. *Mol Cancer Ther* **2**:131-8.

Molecular Pharmacology Fast Forward. Published on July 6, 2006 as DOI: 10.1124/mol.106.025643
This article has not been copyedited and formatted. The final version may differ from this version.

Footnotes

This work was supported by National Institute of Health grant R01-CA51210

Address correspondence to: Dr David Ross, department of Pharmaceutical sciences, School of Pharmacy, University of Colorado at Denver and Health Sciences Center, 4200 East 9th Ave., Denver, CO 80262 USA. e-mail: david.ross@uchsc.edu

† These authors contributed equally to this work.

Molecular Pharmacology Fast Forward. Published on July 6, 2006 as DOI: 10.1124/mol.106.025643
This article has not been copyedited and formatted. The final version may differ from this version.

Scheme 1. The NQO1 mediated reduction of the benzoquinone ansamycin Hsp90 inhibitors.

Scheme 2. A proposed model of prodrug delivery of the hydroquinone ansamycins and the maintenance of the hydroquinone form of the Hsp90 inhibitor by NQO1.

Figure 1. HPLC and LC-MS analysis of the reduction of 17DMAG by NQO1 to 17DMAGH$_2$.
HPLC analysis of the rhNQO1-mediated reduction of (A) 17DMAG to (B) 17DMAGH$_2$ and inhibition of this reduction by (C) ES936. (A) 17DMAG and NADH; (B) 17DMAG, NADH, and rhNQO1; (C) 17DMAG, NADH, rhNQO1, and ES936 (1 μmol/L). Reaction conditions: 20 μmol/L 17DMAG, 500 μmol/L NADH, and 6.6 μg rhNQO1 in 50 mmol/L potassium phosphate buffer (pH 7.4; 1 mL) containing 1 mg/mL BSA. After 30 minutes, the internal standard N-phenyl-1-naphthylamine (10 μg/mL) was added, the sample centrifuged and the supernatant was analyzed immediately by HPLC at 270 nm. (D) LC-MS confirmed 17DMAGH$_2$ as the product of NQO1-mediated reduction of 17DMAG.

Figure 2. Inhibition of yeast Hsp90 by the benzoquinone ansamycins.
Yeast Hsp90 ATPase activity was measured in reactions with either vehicle (DMSO) or the appropriate benzoquinone ansamycin in the presence and absence of rhNQO1, the reactions were analyzed after 3 hours. Phosphate concentrations were measured using the malachite green assay. Open columns, the benzoquinone ansamycin and NADH; filled columns, the benzoquinone ansamycin, NADH, and NQO1; hatched columns, the benzoquinone ansamycin, NADH, NQO1, and ES936. Columns, mean (n = 3); bars, SD. Hsp90 ATPase activity in incubates containing the benzoquinone ansamycin, NADH, and NQO1 were statistically different from incubates containing either the benzoquinone ansamycin and NADH or the benzoquinone ansamycin, NADH, NQO1, and ES936, *, $P < 0.05$, one-way ANOVA with Tukey for pairwise comparison.

Figure 3. HPLC analysis of 17DMAGH$_2$ formation by MDA468 and MDA468/NQ16 cell sonicates.
HPLC analysis confirmed the formation of 17DMAGH$_2$ following reduction of 17DMAG by MDA468/NQ16 cell sonicates. (A) 17DMAG, NADH, and MDA468 cell sonicates; (B) 17DMAG, NADH, and MDA468/NQ16 cell sonicates; (C) 17DMAG, NADH, and MDA468/NQ16 cell sonicates and ES936 (1 μmol/L). Reaction conditions: 20 μmol/L 17DMAG, 500 μmol/L NADH, and 500 μg of cell sonicate in 50 mmol/L potassium phosphate buffer (pH 7.4; 1 mL) containing 1 mg/mL BSA. After 30 minutes, the internal standard N-phenyl-1-naphthylamine (10 μg/mL) was added, the sample centrifuged and the supernatant was analyzed immediately by HPLC at 270 nm.

Figure 4. Effect of 17DMAG on growth inhibition and Hsp90 client proteins in human breast cancer cells.
Growth inhibition following 17DMAG treatment was measured by MTT analysis in (A) MDA468 (NQO1-null) and (B) MDA468/NQ16 (high NQO1) cell lines in the presence (filled symbols) and absence (open symbols) of ES936. Points, mean (n = 3); bars, SD. The effect of exposure time on the fold potentiation of (C) 17AAG and (D) 17DMAG growth inhibition in MDA468 and MDA468/NQ16 cells. IC_{50} values were measured in MDA468 and MDA468/NQ16 cells after exposure to 17AAG or 17DMAG for 4hr and 72hr time periods. Data is expressed as the ratio of the IC_{50} for MDA468 cells divided by the IC_{50} for MDA468/NQ16 cells. (E) The effect of 17DMAG on Hsp70 and Raf-1 protein levels. Hsp70 and Raf-1 protein levels were analyzed by immunoblot analysis after treatment of MDA468 and MDA468/NQ16 cells with 17DMAG for 24 hours. Hsp70 immunoblot analysis was performed on 10 μg whole-cell sonicate. Raf-1 immunoblot analysis was performed on 100 μg whole-cell sonicate. Results were confirmed in duplicate experiments.

Figure 5. Molecular modeling of the N-terminal of the yeast Hsp90-17DMAG/17DMAGH$_2$ complex.
Flat ribbon representation of the yeast Hsp90 ATP-binding domain with (A) 17DMAG and (B) 17DMAGH$_2$ and stick display style representation of the key interactions with (C) 17DMAG and (D) 17DMAG all figures display hydrogen bond contacts (blue dashed lines) with amino acid residues and water molecules (colored by atom type, except ligand carbons atoms which are colored yellow). The figures were constructed using Discovery Studio Viewer Professional Software (Accelrys, Inc., San Diego, CA).

Molecular Pharmacology Fast Forward. Published on July 6, 2006 as DOI: 10.1124/mol.106.025643
This article has not been copyedited and formatted. The final version may differ from this version.

Compound	IC_{50}(μM)				IC_{50} Fold Difference
	MDA468	MDA468+ES936	NQ16	NQ16+ES936	
GM	0.063±0.011	0.064±0.013	0.023±0.0003	0.057±0.01	3
17AAG*	10.05±1.07	7.34±1.04	0.86±0.16	7.67±1.36	12
17AG	6.77±0.77	6.62±0.42	1.1±0.11	5.61±1.05	6
17DMAG	2.06±0.25	1.9±0.19	0.22±0.05	1.81±0.2	9
17AEP-GA	2.69±0.08	2.68±0.12	0.65±0.04	2.59±0.18	4
Radicicol*	3.81±0.44	---	4.04±0.35	---	1

Table 1. Growth inhibition effect of a series of Hsp90 inhibitors in MDA468 and MDA468/NQ16 cells following treatment (4 hours).

* Data for 17AAG and radicicol has been reported previously (Guo et al., 2005).

Molecular Pharmacology Fast Forward. Published on July 6, 2006 as DOI: 10.1124/mol.106.025643
This article has not been copyedited and formatted. The final version may differ from this version.

Compound	E_{vdw} (kcal/mol)	E_{elect} (kcal/mol)	E_{total} (kcal/mol)	H-Bond Interaction		H-Bond Distance (Å)
				Amino Acid / Solvent	Ligand	
17DMAG	-26.5	-27.7	-54.2	ASP-79	Carbamate NH_2	2.04
				LYS+98	Quinone C=O	1.74
				HOH400	Carbamate C=O	2.14
				HOH402	Carbamate NH_2	2.22
				HOH403	Methoxy (ansa) OCH_3	2.35
				HOH403	Carbamate R-O-$CONH_2$	2.18
				HOH405	Hydroxy (ansa) OH	2.32
				HOH407	Quinone C=O	1.65
				HOH485	Amine R-N$(CH_3)_2$	1.95
				HOH529	Amide NH	1.95
$17DMAGH_2$	-30.9	-28.1	-58.9	ASP-40	Hydroquinone O-H	2.00
				ASP-79	Carbamate NH_2	1.86
				PHE124	Amide C=O	2.14
				HOH400	Carbamate C=O	1.99
				HOH402	Carbamate NH_2	2.35
				HOH403	Methoxy (ansa) OCH_3	2.38
				HOH405	Hydroxy (ansa) OH	1.93
				HOH529	Amide NH	2.07

Table 2. Total interaction energy, van der Waals, electrostatic energy, and hydrogen bonding interactions between yeast Hsp90 and 17DMAG/$17DMAGH_2$.

Molecular Pharmacology Fast Forward. Published on July 6, 2006 as DOI: 10.1124/mol.106.025643
This article has not been copyedited and formatted. The final version may differ from this version.

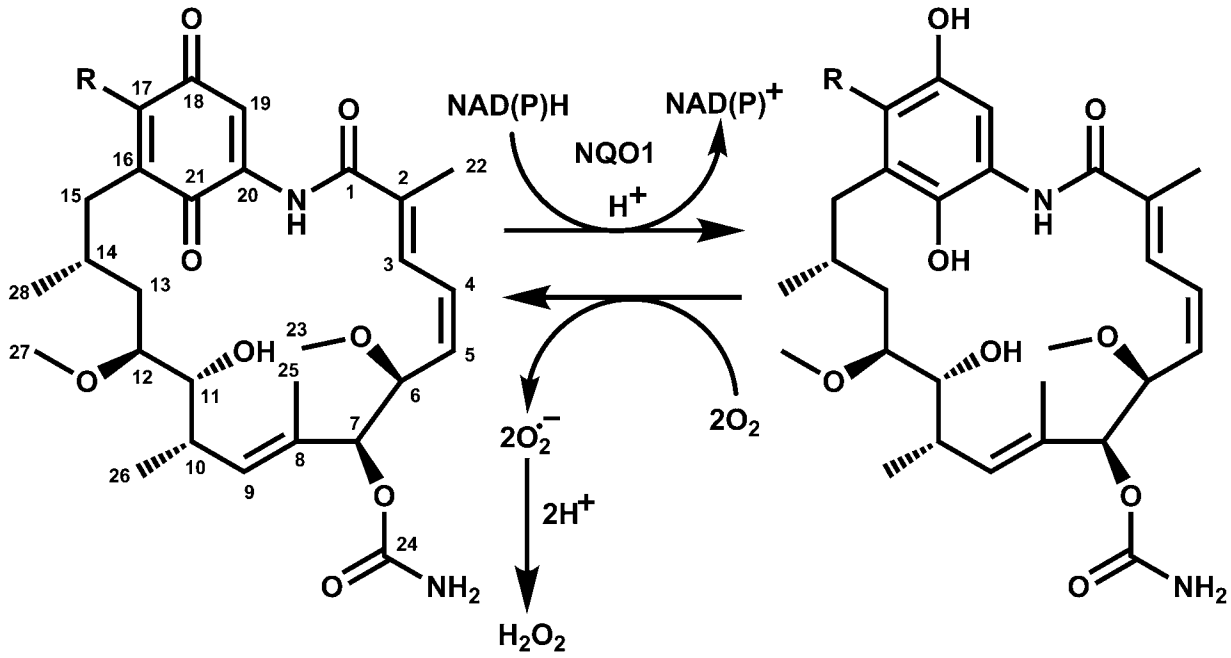

Compound	R (17-Substitutent)	MW
GM	OCH_3	560
17AAG	$NHCH_2CHCH_2$	586
17AG	NH_2	545
17DMAG	$NHCH_2CH_2N(CH_3)_2$	616
17AEP-GA	$NHCH_2CH_2NC_4H_8$	643

Scheme 1.

Molecular Pharmacology Fast Forward. Published on July 6, 2006 as DOI: 10.1124/mol.106.025643
This article has not been copyedited and formatted. The final version may differ from this version.

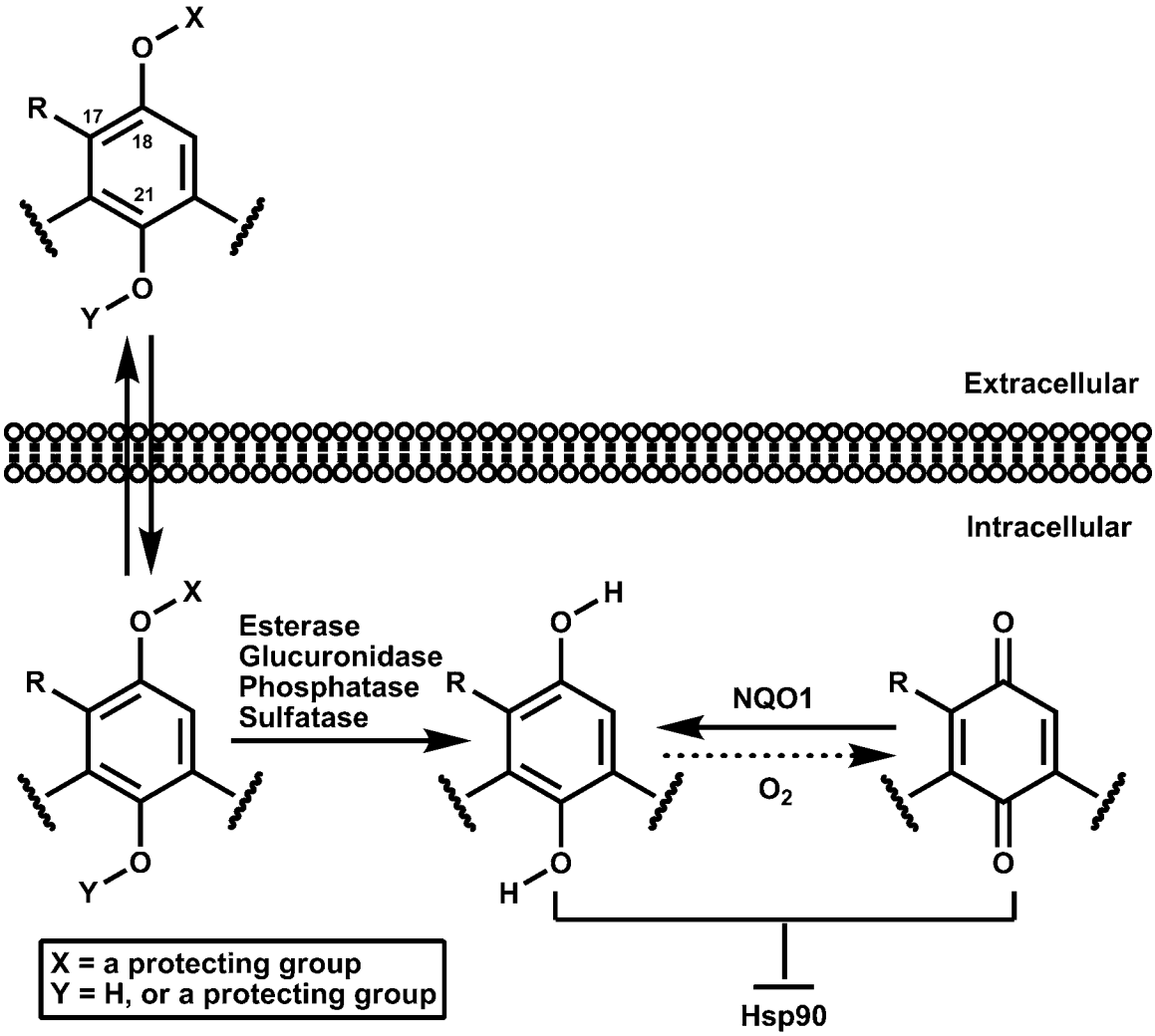

Scheme 2.

Molecular Pharmacology Fast Forward. Published on July 6, 2006 as DOI: 10.1124/mol.106.025643
This article has not been copyedited and formatted. The final version may differ from this version.

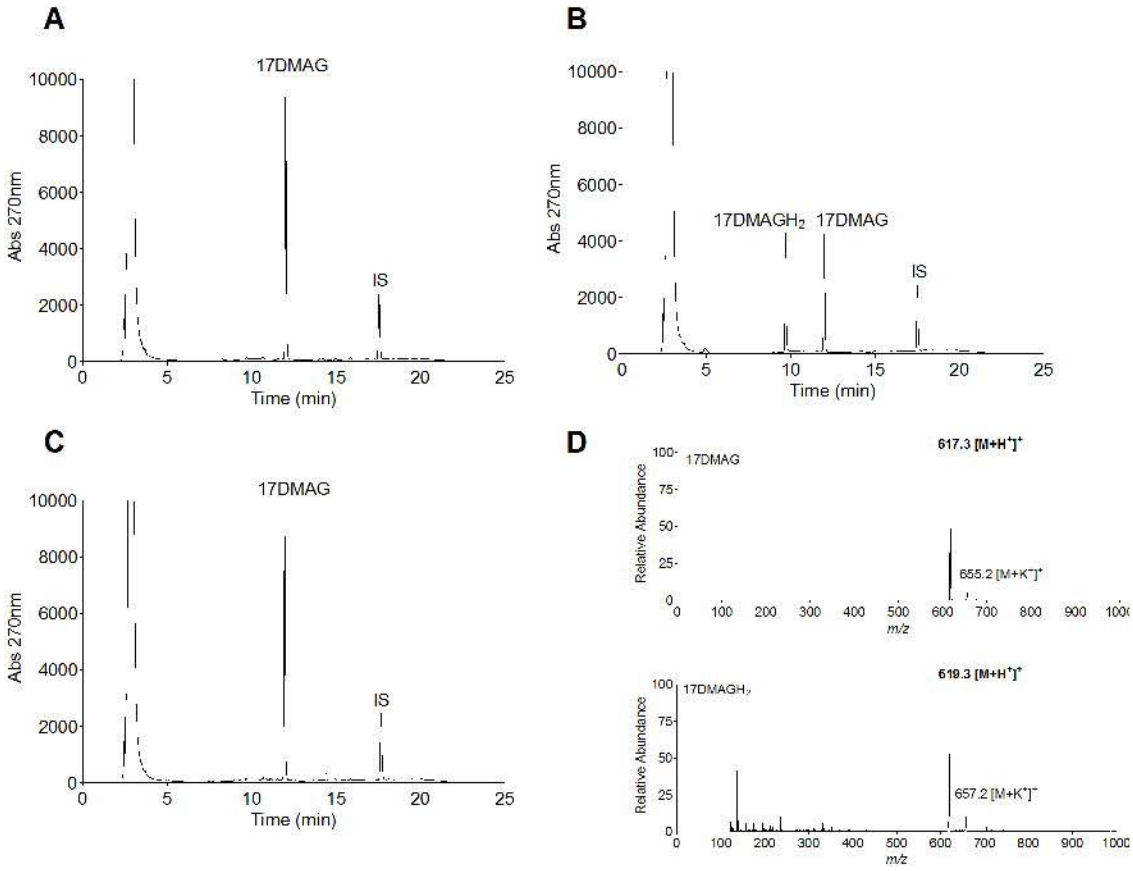

Figure 1.

Molecular Pharmacology Fast Forward. Published on July 6, 2006 as DOI: 10.1124/mol.106.025643
This article has not been copyedited and formatted. The final version may differ from this version.

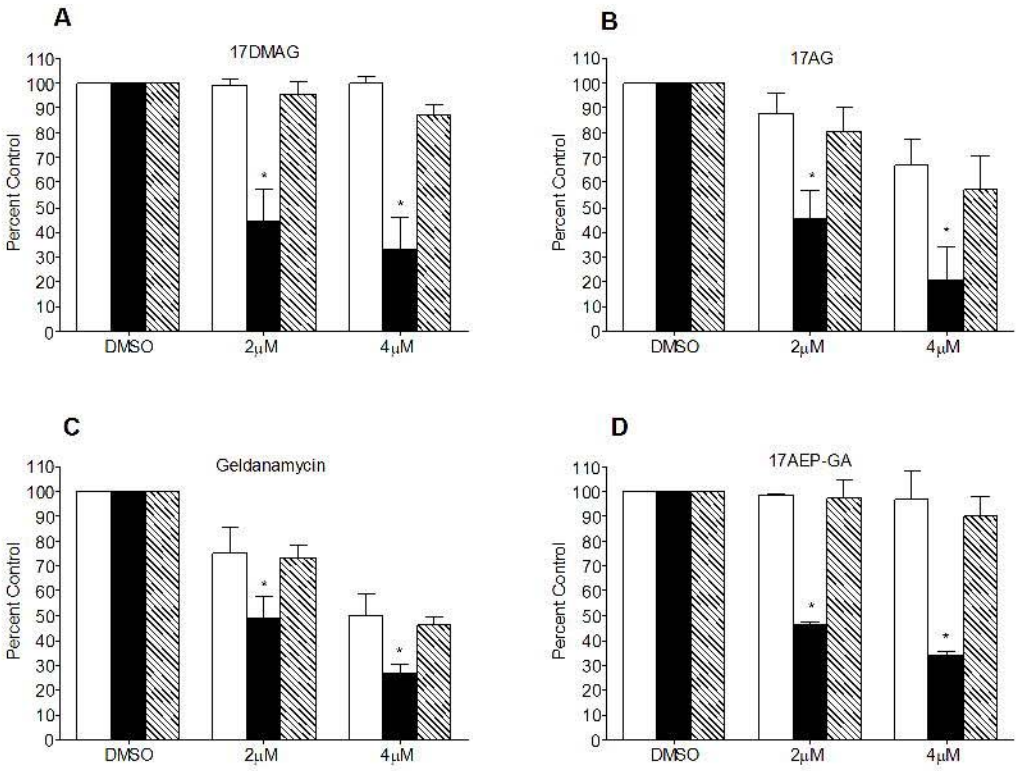

Figure 2.

Molecular Pharmacology Fast Forward. Published on July 6, 2006 as DOI: 10.1124/mol.106.025643
This article has not been copyedited and formatted. The final version may differ from this version.

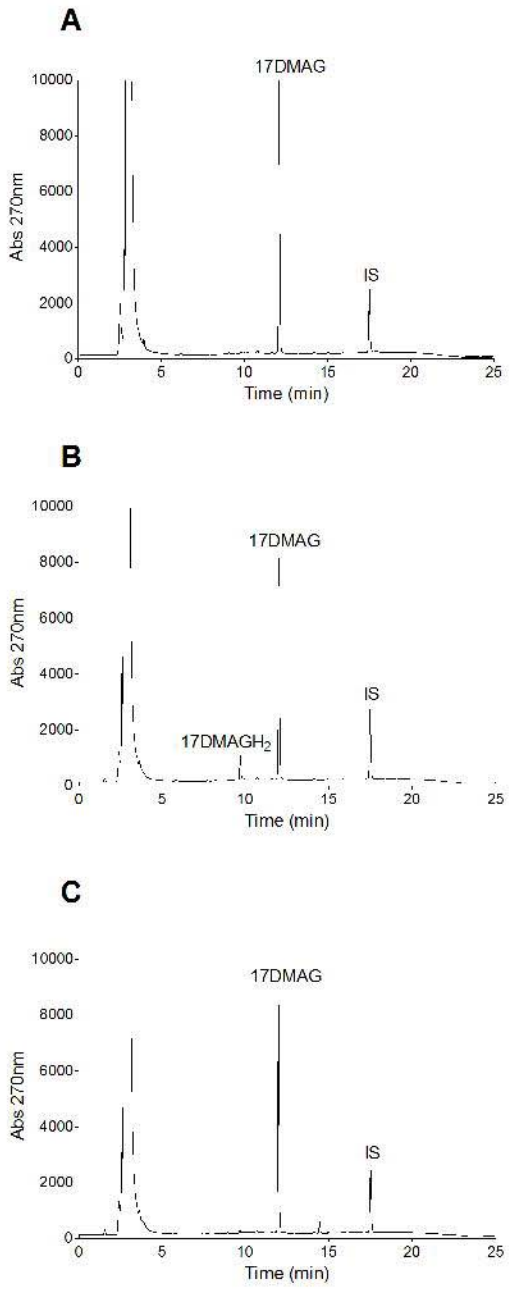

Figure 3.

Molecular Pharmacology Fast Forward. Published on July 6, 2006 as DOI: 10.1124/mol.106.025643
This article has not been copyedited and formatted. The final version may differ from this version.

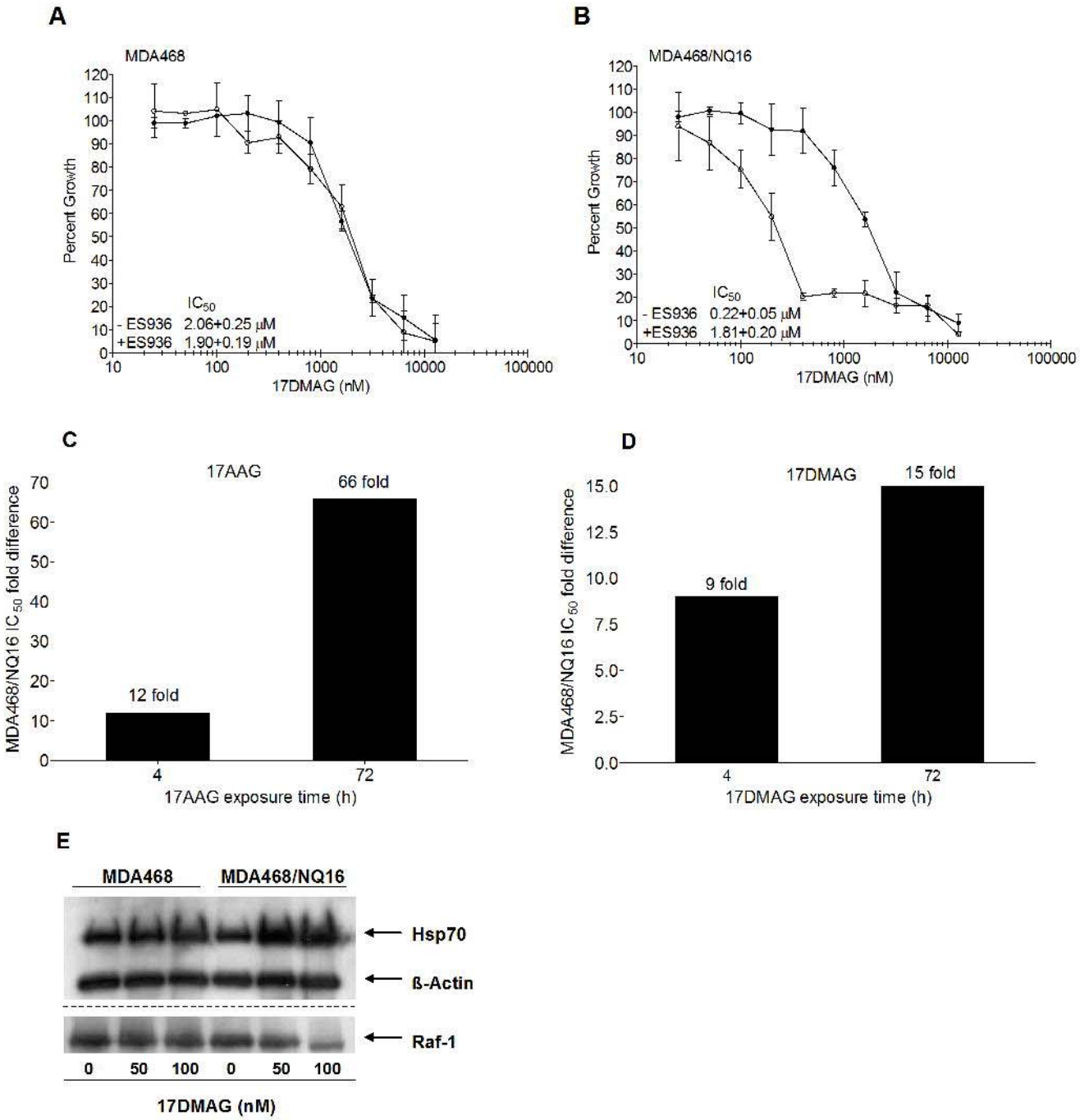

Figure 4.

Molecular Pharmacology Fast Forward. Published on July 6, 2006 as DOI: 10.1124/mol.106.025643
This article has not been copyedited and formatted. The final version may differ from this version.

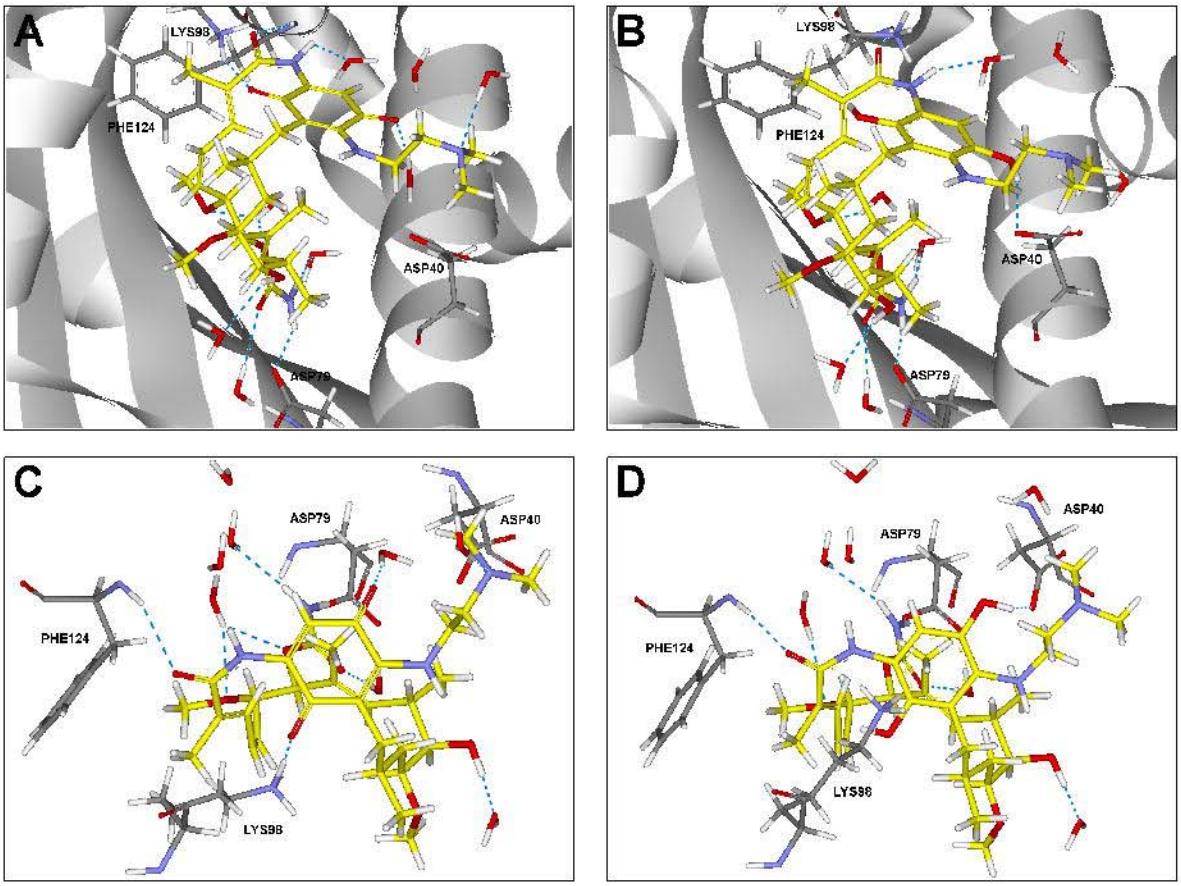

Figure 5.